Correlations between diffusion, internal magnetic field gradients, and transverse relaxation in porous systems containing oil and water

John Georg Seland*
Department of Circulation and Medical Imaging, Norwegian University of Science and Technology, N-7489 Trondheim, Norway

Kathryn E. Washburn
Department of Physics, Norwegian University of Science and Technology, N-7401 Trondheim, Norway

Henrik W. Anthonsen and Jostein Krane
Department of Chemistry, Norwegian University of Science and Technology, N-7491 Trondheim, Norway
(Received 1 March 2004; published 11 November 2004)

The main focus in this study is to investigate the correlations between internal magnetic field gradients (G_0) and transverse relaxation times in liquid-saturated packings of glass beads of different wettabilities. We show how these correlations can be expressed as two-dimensional (2D) diagrams of distribution functions between internal magnetic field gradients and T_2 values. In the case where it is difficult to distinguish the signals from oil and water, we separate them based on their difference in diffusivity. In addition to using such diffusion weighting in the G_0-T_2 diagrams, we also show results from experiments where the direct correlation between diffusion and T_2 (D-T_2) is determined. The overall results show that the wettability of the glass beads has a strong influence on the appearance of these diagrams, in particular on the location of the fast diffusing water molecules. However, due to their lower diffusivity, the transverse magnetization of the oil molecules is not so greatly influenced by either the presence of the glass beads or their wettability properties. Thus, the wettability properties of a liquid-filled porous material can be determined from the location of the water signal in such 2D diagrams. In particular, we show that this is the case not only for D-T_2 diagrams, but also for G_0-T_2 diagrams.

DOI: 10.1103/PhysRevE.70.051305 PACS number(s): 81.05.Rm, 82.56.Lz, 82.56.Na, 76.60.Es

INTRODUCTION

Relaxation processes of spin bearing molecules in liquid-saturated porous materials are influenced by the physical and chemical surroundings. We focus on the transverse component of the magnetization in the rotating frame of reference, and in the usual manner we define $M^+ = M_x + iM_y$. We also take into consideration that there might be an offset in the resonance frequency, which we express as $\Delta\omega(t) = \gamma(g(t)\cdot r)$, where $g(t)$ in the general case is a time and spatial dependent magnetic field gradient across the sample, and γ is the gyromagnetic ratio. The gradient can be either an internal magnetic field gradient induced by susceptibility differences in the sample, or an external applied gradient. The governing equation for the evolution of the transverse magnetization is given by [1]

$$\frac{\partial M^+(r,t)}{\partial t} = D\nabla^2 M^+(r,t) - \frac{M^+(r,t)}{T_2} - i\gamma(g(t)\cdot r)M^+(r,t) \tag{1}$$

where D is the molecular diffusion coefficient, and T_2 is the transverse relaxation time. The solution to Eq. (1) can be written as [2]

$$M^+(r,t) = M_0(r)\exp\left[-\frac{t}{T_2} - \gamma^2 D\int_0^t\left(\int_0^{t'} g(t)dt''\right)^2 dt'\right] \tag{2}$$

where $M_0(r)$ is the total magnetization at thermal equilibrium.

In a porous system, the spins will relax at the surface, leading to an additional sink of the magnetization [3]

$$\hat{n}\cdot D\nabla M^+(r,t) + \rho_2 M^+(r,t)|_S = 0 \tag{3}$$

where $\hat{n}$ is the unit outward normal on the solid/fluid interface, and ρ_2 is a parameter known as the surface relaxation strength. The subscript $|_S$ indicates the surface boundary condition.

In the absence of a magnetic field gradient and with no surface relaxation, the transverse relaxation rate is solely given by the bulk liquid relaxation processes, and one observes, if we have a pure liquid, the usual monoexponential behavior of the T_2 decay. If we include surface relaxation, and the rate determining step is relaxation at the surface, the transverse relaxation rate in a single pore can be written as [3,4]

$$\frac{1}{T_2} = \frac{1}{T_2^{bulk}} + \rho_2\frac{S}{V} \tag{4}$$

where T_2^{bulk} is the transverse relaxation time in the bulk liquid, and S/V is the surface-to-volume ratio of the pore. In a system having a distribution of pore sizes with different

*Electronic address: john.seland@medisin.ntnu.no

surface-to-volume ratios there will also be a corresponding distribution of relaxation times. The total magnetization, integrated over the total volume of the sample, is then given by

$$M(t) = \int M^+(r,t)d^3r = \int \rho(T_2)e^{-t/T_2}dT_2 \tag{5}$$

where $\rho(T_2)$ represents a distribution of T_2 values within the sample.

We have not yet taken into account magnetic field gradients across the sample. When a fluid-saturated porous sample is placed in an external, homogeneous magnetic field, differences in magnetic susceptibility between solid grains and pore fluid may induce large local field inhomogeneities inside the pores, known as internal magnetic field gradients, or susceptibility gradients. Diffusion of spin bearing molecules in these susceptibility gradients leads to a magnetic phase grating across the sample, and will introduce additional dephasing of transverse magnetization in the Hahn echo sequence [5].

The dynamics of the transverse magnetization as measured in a Carr-Purcell-Meiboom-Gill (CPMG) experiment [5,6] can be calculated from Eq. (2). We introduce the wave number $k(t)=\gamma\int_0^t g(t')dt'$, which defines the magnetic phase grating in the sample [7]. We now include both effects from surface relaxation and internal magnetic field gradients. Equation (2) can then be rewritten as

$$M^+(r,t) = M_0(r)e^{-t/T_2}\exp\left(-D\int_0^t k(t)^2dt\right). \tag{6}$$

The solution to this equation is given by integrating over the various time intervals in the CPMG sequence, and then over the total volume of the sample. We assume a time independent internal magnetic gradient G_0 over the sample, leading to a phase grating given by $k(t)=\int_0^t G_0dt'$. The magnetization of echo number n is then given by

$$M(r,2n\tau) = \int M^+(r,2n\tau)d^3r = \int M_0(r)e^{-2n\tau/T_2}e^{-Dk_0^2 2n\tau/3}d^3r \tag{7}$$

where 2τ is the spacing between echoes in the CPMG train, and $k_0=\gamma G_0\tau$. From the previous considerations we know that the volume integration over the first exponential term can be related to a distribution of T_2 values. The second term represents the well known additional dephasing of the magnetization due to diffusion in internal gradients. We could assume a spatial distribution of internal gradients over the sample, $P(G_0)$, and rewrite Eq. (7) as

$$M(2n\tau) = \int \rho(T_2)e^{-2n\tau/T_2}dT_2 \int P(G_0)e^{-D\gamma^2{G_0}^2\tau^2 2n\tau/3}dG_0. \tag{8}$$

Knowledge about the relationship between transverse relaxation and internal gradients can be used for a better understanding of the influence of internal gradients on transverse relaxation times. In addition, as we will show in this paper, it can also act as a diagnostic tool for the determination of the wettability properties of the surface in a porous material. However, the relationship between the distribution of internal gradients and the distribution of T_2's, as measured in an ordinary CPMG measurement, is very complex. We can measure the T_2 decays as a function of different echo spacing τ, and then try to invert these attenuations along the "direction" of these varying τ values, but as explained in [8] this will not give the desired result. The reason is that the time interval $2n\tau$ in the second exponential term is not separable from the echo train, and the inverted amplitudes will not be given by Eq. (8). Thus, the time interval where the dephasing due to internal gradients is taking place has to be decoupled from the time interval where T_2 relaxation is occurring.

Recently it was shown that by using a two-dimensional (2D) internal gradient–transverse relaxation experiment it is possible to extract the correlated distribution function between internal gradients and transverse relaxation times in a multiple pore scale system [8]. Similar approaches for determination of 2D distribution functions between diffusion and relaxation have also recently been suggested [9,10]. In both types of experiments the spins are diffusion encoded in a preparation interval before being detected in a CPMG measurement. In the case of correlation between internal gradients and transverse relaxation, the preparation interval is a CPMG train with a varying number of π pulses applied in the presence of internal gradients, while for correlations between diffusion and transverse relaxation the preparation interval is a spin echo or stimulated echo sequence performed in an inhomogeneous B_0 field. In both cases the spins are encoded for different degrees of dephasing due to molecular diffusion in inhomogeneous fields.

In a previous paper [11] we showed that by using diffusion encoded CPMG measurements, it is possible to separately measure the T_2 attenuation of oil and water in a system where strong internal magnetic field gradients make it difficult to separate these signals due to their difference in chemical shift. In those measurements pulsed field gradients were applied in the diffusion encoding of the spins, making it possible to attenuate the water signal to a level where one is left with signal from oil only, which is a necessary criterion for a total separation of the two signals.

In the present paper we combine the method for measurements of 2D distribution functions between internal gradients and transverse relaxation with the method for separation of oil and water signals. It is then possible to measure the distribution functions between internal gradients and transverse relaxation times separately for oil and water simultaneously present in a porous system. This makes it possible to identify which phase is wetting the surface of the porous material.

THEORY

In an ordinary CPMG measurement it is impossible to determine a useful relationship between the distribution of internal gradients and the distribution of T_2 values. Instead, we follow the approach of Sun and Dunn [8], split the CPMG sequence into two parts, and perform a 2D experiment, as shown in Fig. 1. By varying the number of π pulses in the first part of the sequence, an encoding for internal

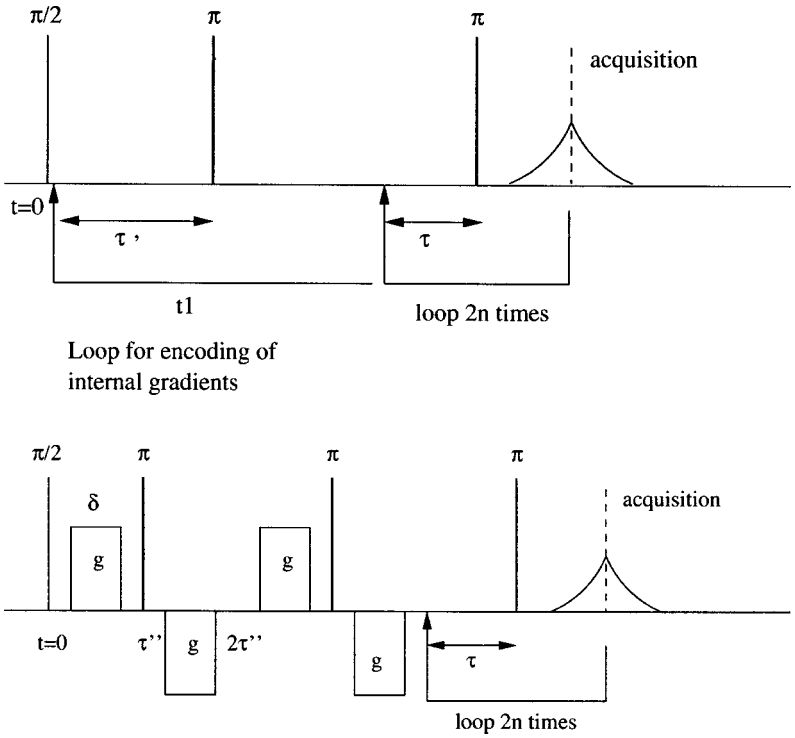

FIG. 1. Two-dimensional pulse sequences for measurements of correlations. (a) Pulse sequence for measurement of correlation between internal gradients and transverse relaxation times [8]. (b) Pulse sequence for measurement of correlations between diffusivity and transverse relaxation times [11].

gradients can be performed. The second part of the sequence is an ordinary CPMG train where the τ value is kept sufficiently short, so that the effect from internal gradients does not have a significant impact. The time interval for encoding of internal gradients and the time interval for T_2 relaxation are now separated from each other. The echo attenuation for this pulse sequence can be expressed as

$$M(\tau',2n\tau) = \int\int f(DG_0^2,T_2)e^{-(t1+2n\tau)/T_2}e^{-D\gamma^2G_0^2\tau'^2 2n'\tau'/3}dT_2d(DG_0^2) \tag{9}$$

where $2\tau'$ is the spacing between π pulses in the first part of the sequence, n' is the number of π pulses, and t_1 is the total length of this internal gradient coding interval. $f(DG_0^2,T_2)$ is a two-dimensional distribution function of "internal gradients" and transverse relaxation times. Note that it is not the actual distribution of internal gradients that is determined, but rather the distribution of the term DG_0^2. If we assume a constant, well defined diffusion coefficient, we can determine the distribution of G_0^2 values, and in this manner we determine the absolute value of the internal gradient as $|G_0|=\sqrt{G_0^2}$. For simplicity we will from now on refer to this as the "internal gradient." The true internal gradient will be spatially dependent, and the value we measure in our experiment will thus depend on how long we allow the liquid molecules to diffuse. This is important to keep in mind when the results are interpreted.

If the diffusivity is not constant over the sample, we cannot use the assumptions described above. This will complicate the analysis in a system where there are liquids with different mobilities present, and when these liquids experience different strengths of the internal gradients. However, by using applied gradients in the encoding interval instead of internal gradients, we can determine the diffusivity. A pulse sequence implementing applied field gradients in front of the CPMG measurement is shown in Fig. 1(b). Bipolar gradients are applied in order to suppress cross terms between applied and internal gradients [12]. We vary the intensity of the applied gradients, and keep all the time intervals constant. The echo attenuation for this sequence is given by

$$M(k,2n\tau) = \int\int f(D,T_2)e^{-(t_e+2n\tau)/T_2}e^{-(k^2t_DD)}dT_2dD \times \int e^{-D\gamma^2G_0^2\tau''^2 4\tau''/3}d^3r \tag{10}$$

where $k=2\gamma g\delta$, $t_e=4\tau''$ is the T_2 relaxation time in the Pulsed Field Gradients (PFG) part of the sequence, and $t_D=3/2\tau''-\delta/6$ is the diffusion time. $f(D,T_2)$ now describes a two-dimensional distribution of diffusion coefficients and transverse relaxation times within the porous system. The integration over the last exponential term represents an attenuation in the signal due to internal gradients, but since the time interval τ'' is kept constant, this term can be treated as an offset.

We now have one sequence where we encode for internal gradients, and one where we encode for diffusivity, before collecting a CPMG train. In Fig. 2 we have combined these two pulse sequences. The pulse sequence is now divided into three parts. The gradient encoding interval is preceeded by a bipolar Pulsed Gradient Spin Echo (PGSE) interval where the intensity of the gradient pulses can be varied. The echo attenuation for this pulse sequence is written as

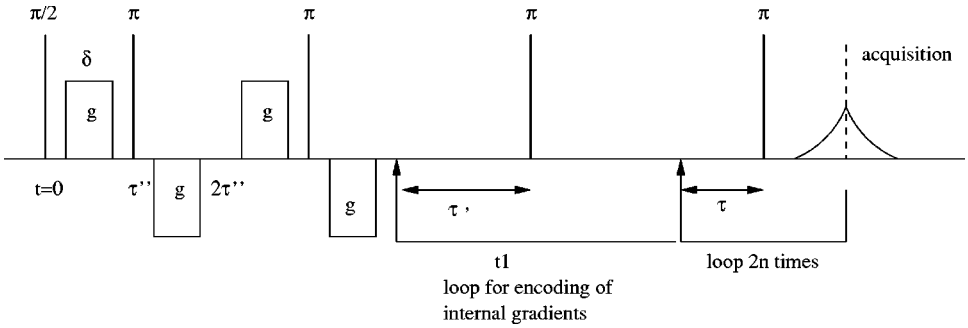

FIG. 2. Pulse sequence for measurement of correlations between diffusivity, internal gradients, and transverse relaxation times.

$$M(k,\tau',2n\tau) = \int\int\int f(D,DG_0^2,T_2)e^{-k^2t_D D}e^{-(t_e+t_1+2n\tau)/T_2} \times e^{-\gamma^2G_0^2(4\tau''\tau''^2+\tau'^2 2n'\tau')D/3}dD\,dT_2\,d(DG_0^2) \tag{11}$$

where $f(D,DG_0^2,T_2)$ now is a three-dimensional distribution function between diffusion, internal gradients, and transverse relaxation time. The constant term due to dephasing in internal gradients in the first diffusion encoding interval has been incorporated in the last exponential term. By varying the intensity of the applied gradients, an encoding for diffusivity can be performed, and this encoding will be independent of internal gradients. In principle we could now perform a 3D experiment and determine the distribution function $f(D,DG_0^2,T_2)$. Instead we choose to use the diffusion encoding to identify and separate the signals from oil and water. In an experiment where the applied gradients are equal to zero, $(k=0)$, the echo attenuation is given by

$$M(0,\tau',2n\tau) = \int\int f'(DG_0^2,T_2)e^{-(t_e+t_1+2n\tau)/T_2}e^{-\gamma^2G_0^2(4\tau''\tau''^2+\tau'^2 2n'\tau')D/3} \times dT_2\,d(DG_0^2) \tag{12}$$

where $f'(DG_0^2,T_2)=\int f(D,DG_0^2,T_2)dD$ is now a 2D distribution function that is equal to the one in Eq. (9), apart from an additional dephasing in internal gradients that will lead to a loss in signal from molecules that experience strong internal gradients. Since the diffusivity of oil is much lower than that of water, we can suppress the signal from water by applying a strong enough gradient in the experiment [11]. The echo attenuation in such an experiment is given by

$$M(k_{supp},\tau',2n\tau) = \int\int f'_{oil}(D_{oil}G_0^2,T_2^{oil})e^{-k_{supp}^2 t_D D_{oil}} \times e^{-(t_e+t_1+2n\tau)/T_2^{oil}}e^{-\gamma^2G_0^2(4\tau''\tau''^2+\tau'^2 2n'\tau')D/3} \times dT_2^{oil}d(D_{oil}G_0^2) \tag{13}$$

where $f'_{oil}(D_{oil}G_0^2,T_2^{oil})$ is a diffusion weighted distribution function for oil only.

If we perform a series of experiments with values of k from k_{supp} and upward, the result will be a series of diffusion weighted signals from oil, and we can use this information to extrapolate the oil attenuation back to the form it was supposed to have at $k=0$, without water present. We then obtain

$$M_{oil}(0,\tau',2n\tau) = \int\int f'_{oil}(D_{oil}G_0^2,T_2^{oil})e^{-(t_e+t_1+2n\tau)/T_2^{oil}} \times e^{-\gamma^2G_0^2(4\tau''\tau''^2+\tau'^2 2n'\tau')D/3}dT_2^{oil}d(D_{oil}G_0^2). \tag{14}$$

This signal can be subtracted from the signal obtained at $k=0$ [Eq. (12)], and the result will be the signal from water,

$$M_{wat}(0,\tau',2n\tau) = M(0,\tau',2n\tau) - M_{oil}(0,\tau',2n\tau) = \int\int f'_{wat}(D_{wat}G_0^2,T_2^{wat})e^{-(t_e+t_1+2n\tau)/T_2^{wat}} \times e^{-\gamma^2G_0^2(4\tau''\tau''^2+\tau'^2 2n'\tau')D/3}dT_2^{wat}d(D_{wat}G_0^2). \tag{15}$$

Following this procedure, we can separate the echo attenuation for oil and water in the system, and by performing a 2D Inverse Laplace Transformation (ILT) on these separated signals, we can determine the 2D distribution functions for oil and water separately.

EXPERIMENT

All the experiments were performed on a Bruker Avance DMX200 instrument, using a commercial diffusion probe from Bruker Biospin (PH MIC DIF 200 WB ^1H SAT 5/10 probe). An applied gradient strength in the range 0–960 G/cm was used. The experiments were performed at a temperature of 25.0±0.5 °C. The pulse sequences in Fig. 1 and Fig. 2 were used. In addition, experiments using an ordinary CPMG sequence was performed for all the samples.

In the CPMG trains the value of τ was set to 0.15 ms. In the internal gradient encoding interval a constant value of $t_1=10.2$ ms was used, and the τ' value was varied from 0.15 to 5.10 ms with a corresponding variation of the number of π pulses from 34 to 1, in 20 steps.

The eddy current delay in the PFG part of the sequence shown in Fig. 2 (the time between the last gradient pulse and the start of the CPMG train) was set to 1.4 ms. The pulse length was 2 ms, and a time interval of 0.1 ms was used between the initial $\pi/2$ pulse and the following gradient pulse, giving a τ'' value of 3.5 ms. In order to verify and control effects from possible eddy currents, we tested the

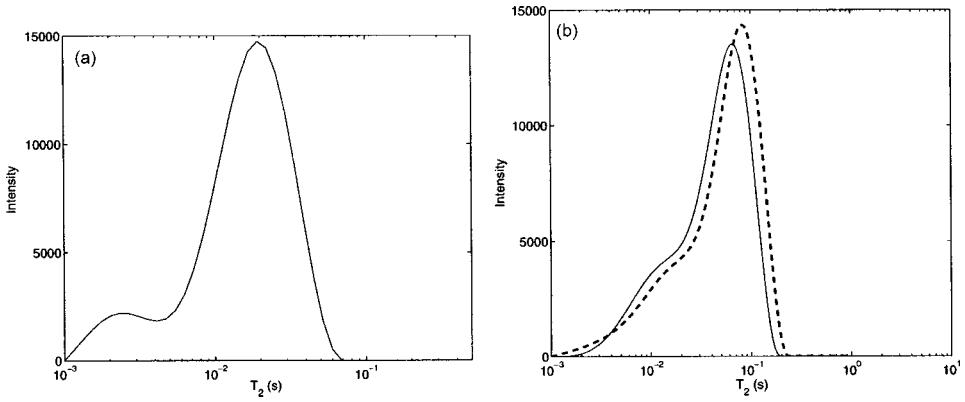

FIG. 3. Separate T_2 distributions of water in water-wet glass beads and oil in oil-wet glass beads. (a) Water in water-wet glass beads. (b) Oil in oil-wet glass beads (−) compared, with bulk oil (--).

sequence on a sample of water doped with $CuSO_4$, which has the same diffusivity as distilled water, but a much shorter T_2 value. We found that under these conditions the transient magnetic fields following the gradient pulses have insignificant effect on the obtained CPMG echo attenuation. For all systems with mobility equal to or lower than that of water, one may then use this set of values.

In the bipolar version of the pulse sequence echo signals from unwanted coherence transfer pathways will be present at the end of the PFG part of the experiment. These unwanted coherences were suppressed by applying a proper phase cycling of the rf pulses and receiver phase [12].

Samples containing water-wet or oil-wet glass spheres immersed in liquids were prepared. The glass spheres were delivered from Duke Scientific, and had a size distribution of 4–60 μm in diameter. The glass spheres are originally water wet. To make the surface of the glass spheres oil wet, the spheres were treated with excess trimethylchlorsilane in a mixed solvent pair of toluene-pyridine kept under an inert atmosphere (argon), and refluxed for several hours. The silated spheres were separated from the solution and washed several times with dichlormethane, and then dried under vacuum at 55 °C.

All the samples were prepared in 10 mm NMR tubes. Samples of distilled water in water-wet glass beads or oil in oil-wet glass beads were prepared by adding 400 μl of liquid, followed by addition of glass beads until there was no bulk liquid present. The oil used was a low sulfur intermediate bunker fuel oil from the Norwegian Esso refinery. The samples of water and oil in water-wet or oil-wet glass beads were prepared by adding aliquots of 200 μl of distilled water and oil to each tube, followed by the addition of 1.40 g of glass spheres (water wet or oil wet). Finally, all the NMR tubes were stirred in an ultrasonic water bath to ensure proper mixing.

The obtained diffusion and relaxation attenuations were analyzed using the two-dimensional inverse Laplace software [13] developed by Callaghan and co-workers at Victoria University of Wellington, New Zealand. This software is based on the algorithm by Venkataramanan *et al.* [14,15].

RESULTS AND DISCUSSION

When a CPMG measurement is preceded by an interval for encoding of internal gradients with the same echo spacing, some of the initial signal may be lost due to relaxation effects, but this should not have a significant impact on the measured T_2 distributions as long as the shortest echo spacing in the preparation interval has the same value as in the CPMG train. Under this condition, the only difference in the two types of experiment lies in where we start the collection of CPMG echoes, and the projection of the distribution onto the T_2 axis should correspond to the original T_2 distribution. However, if the CPMG measurement is preceded by a diffusion encoding interval, we may also expect to see an effect from dephasing in internal gradients. The τ'' value for the experiments performed is 2.1 ms, and if the internal gradients are strong, as we can expect them to be in the systems studied here, this will lead to a significant dephasing of the magnetization before signal is acquired in the CPMG train.

In Fig. 3(a) the T_2 distribution for water in water-wet glass beads, determined using an ordinary CPMG measurement, is shown. The water molecules will be in the fast diffusion limit, and will interact strongly with the surface. This results in a T_2 distribution having a mean value around 20 ms, which is much lower than the bulk relaxation time for distilled water, which is known to be several seconds. The corresponding T_2 distribution for oil in oil-wet glass beads is shown in Fig. 3(b). The T_2 distribution for bulk oil is shown as a comparison, and it is almost similar to the distribution for oil confined in the oil-wet glass beads. This indicates that the relaxation behavior of oil is not strongly influenced by the surface of the glass beads. We performed 2D diffusion-T_2 experiments in bulk oil and oil immersed in oil-wet glass beads. The results are shown in Fig. 4. The main peak for bulk oil is located around 4×10^{-7} cm^2 s^{-1}, with a T_2 value corresponding to the main peak in Fig. 3(b). For oil in oil-wet glass beads, the diffusivity is slightly lower than in bulk, but the T_2 distribution is the same, as was observed in the ordinary CPMG experiment.

When both oil and water are added to the water-wet glass beads [Fig. 5(a)], we clearly see two peaks appear in the T_2 distribution, but they are strongly overlapping, and it is difficult to exactly determine where in the distribution oil and water are found. When the CPMG measurement is preceded by a diffusion encoding interval, we see that a lot of signal is lost before the echoes are collected. Some of the signal loss is explained by the fact that the diffusion encoding sequence is based on the stimulated echo which, because only half of the spins are stored by the second $\pi/2$ pulse, has half the

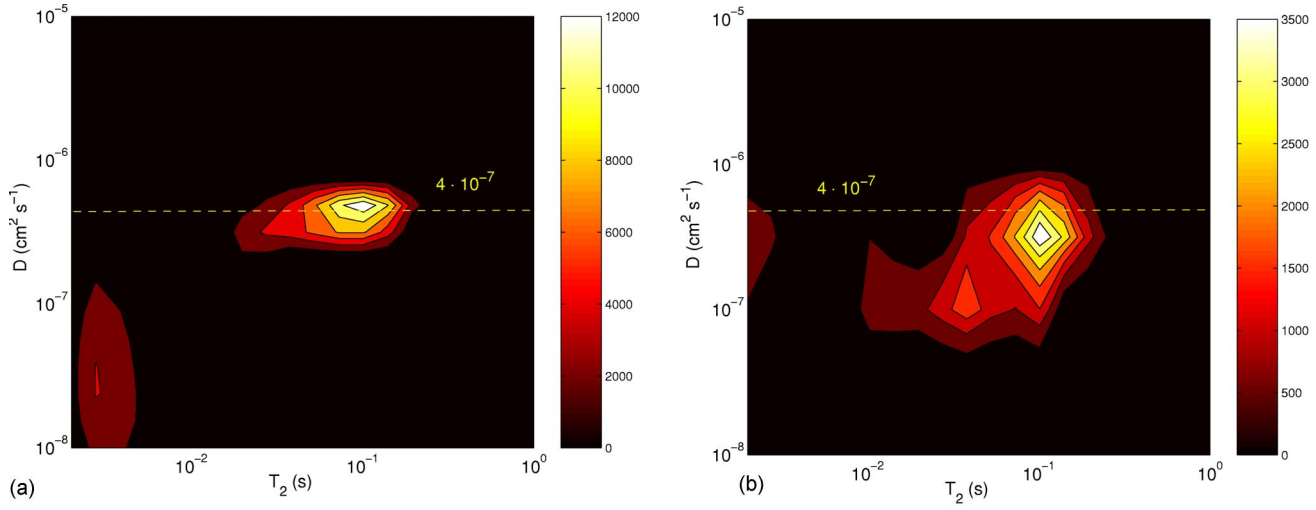

FIG. 4. (Color online) Diffusion-T_2 distributions for bulk oil and oil in oil-wet glass beads. The data were collected using the pulse sequence in Fig. 1(b). The dashed line indicates the mean diffusivity of bulk oil. (a) Bulk oil. (b) Oil in oil-wet glass beads.

intensity of the spin echo. However, taking this into account, we see that a lot of the signal assumed to be mainly associated with water, having T_2 values around 10^{-2} s, is lost due to dephasing of molecules diffusing in internal gradients.

When oil and water are added to the oil-wet glass beads [Fig. 5(b)], two peaks appear in the distribution. The two peaks are not overlapping so strongly as in the water-wet glass beads, but even in this situation we do not know if any of the water signal is hidden under the oil peak, or vice versa. In addition, we have no information about the strength of internal gradients the oil and water molecules experience in the two different samples. Also, here signal is lost when the diffusion weighting interval is applied. It is mostly signal believed to be associated with oil that is lost, indicating that oil molecules experience stronger internal gradients in this sample compared to the water-wet system.

In Fig. 6 the 2D distributions between T_2 and diffusivity for oil and water in water-wet and oil-wet glass beads are shown. In both figures we can easily identify the signals from oil and water, based on their difference in diffusivity. In the water-wet glass beads water has a diffusivity of 1×10^{-5} cm^2 s^{-1}, which is lower than the bulk value of 2.3×10^{-5} cm^2 s^{-1}. The corresponding T_2 value is 20 ms, which is in accordance with the main peak in Fig. 3(a). The oil peak is located at 4×10^{-7} cm^2 s^{-1}, a value that is equal to the measured bulk value for the type of oil used here. The main peak is located at a T_2 value of approximately 80 ms, but some oil is also found at lower relaxation times.

In the oil-wet glass spheres, the oil peak is located at 2×10^{-7} cm^2 s^{-1}, which is lower than in the water-wet sample. This indicates that the diffusion of oil in this sample is more restricted compared to what is observed in the water-wet sample. The diffusivity of water, however, is very close to its bulk value, and the corresponding T_2 value is 1.4 s, which indicates that the properties of water are close to the ones found in bulk liquid.

If we compare the diagrams in Fig. 6 with the distributions in Fig. 5, we can partly, but not clearly, identify which areas in these distributions belong to water and which belong to oil. Thus, this shows how difficult, if not impossible, it is to identify oil and water in one-dimensional distributions like the ones in Fig. 5.

The results from the D-T_2 correlation experiments clearly show that water and oil can be separated based on their difference in diffusivity, making it possible to determine the environment in which oil and water molecules are found, based on such diagrams. Similar results have been obtained by others [9,10]. Let us now take a look at the 2D distributions obtained by applying the "internal gradient–T_2" ($G0$-$T2$) pulse sequence with varying number of π pulses in

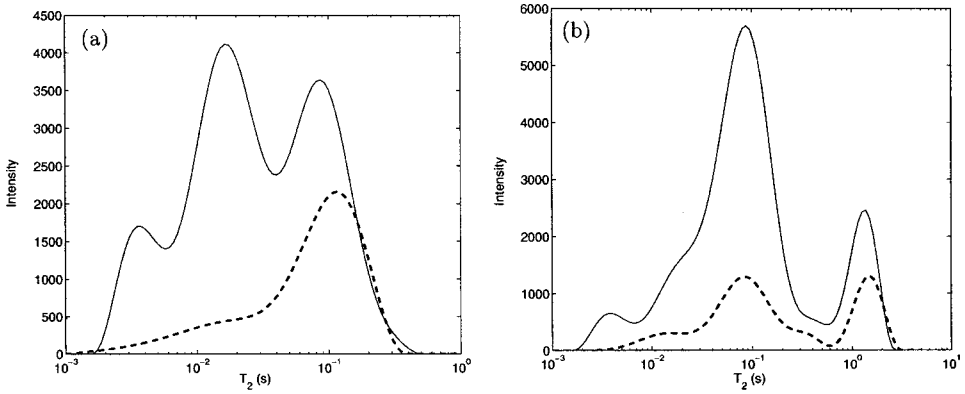

FIG. 5. Measured T_2 distributions for mixtures of oil and water in water-wet and oil-wet glass beads. Ordinary CPMG measurement (−), and with diffusion weighting ($k=0$) in front of the CPMG measurement (--). (a) Water and oil in water-wet glass beads. (b) Water and oil in oil-wet glass beads.

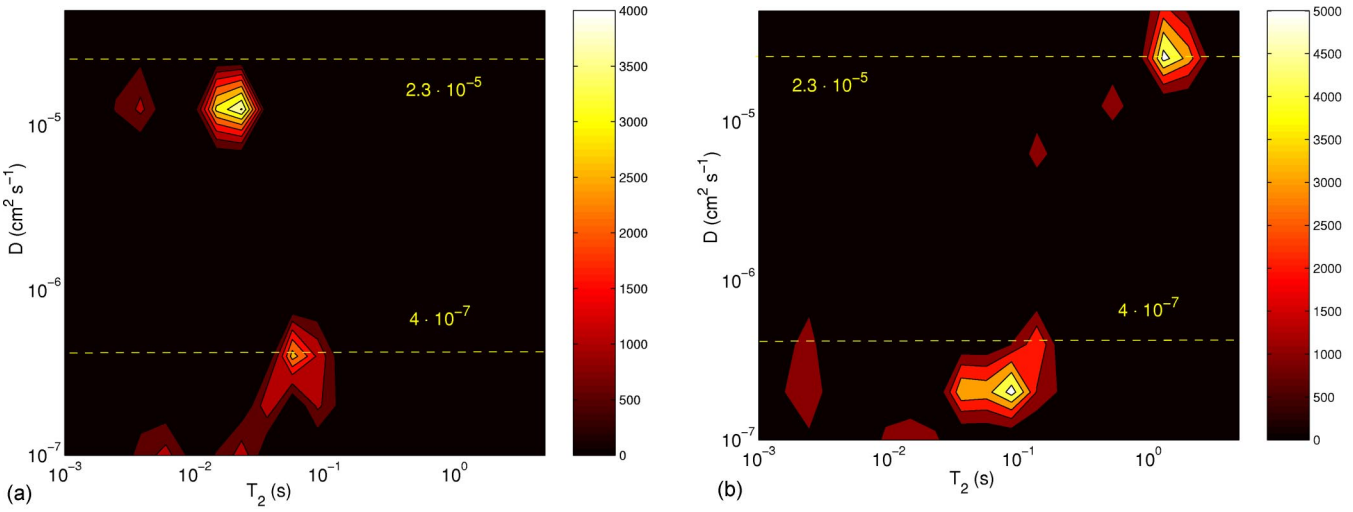

FIG. 6. (Color online) Diffusion-T_2 distributions for oil and water in glass beads (4–60 μm). The data were collected using the pulse sequence in Fig. 1(b). The dashed lines indicate the mean diffusivity for bulk oil and water, respectively. (a) Water and oil in water-wet glass beads. (b) Water and oil in oil-wet glass beads.

the encoding interval. In Fig. 7(a), the result from such a *G*0-*T*2 experiment of water only in water-wet glass beads is shown. We clearly see that the signal is spread out along the vertical direction. We have assumed a constant diffusivity for water equal to 1×10^{-5} cm^2 s^{-1}, and the right side of the vertical axis is normalized with respect to this diffusivity. Clearly, there is a distribution of internal gradients in this sample, and it is correlated with the T_2 distribution. The mean value of the internal gradient is around 300 G/cm. An extrapolation of the data onto the T_2 axis corresponds to the distribution in Fig. 3(a). There is a clear tendency of low values of T_2 to be associated with high internal gradients, but it is interesting to observe that some of the water signal with a T_2 value around 200–300 ms is associated with the strongest internal gradients.

It should be noted that Callaghan *et al.* [13] have determined diffusion-T_2 correlations for molecules confined in simple pore structures, and they showed that there are distinctive areas in the D-T_2 diagrams, depending on the Brownstein-Tarr modes [3]. In one area diffusion is strongly correlated with relaxation, and in the other area the diffusion coefficient may vary independently of relaxation. The secondary peaks in our D-T_2 and G_0-T_2 diagrams may be due to the effects described by Callaghan *et al.* However, the pore structure in our systems is very complex, and since we also consider this to be outside the scope of this paper, we have chosen not to focus on these effects in our paper.

In Fig. 7(b) the 2D distribution of oil and water simultaneously present in water-wet glass beads is shown. The diffusivity of water is much higher than that of oil, which will have a strong impact along the vertical axis, and the signals from oil and water can be separated by pure visual inspection. If we compare this distribution with the 2D distribution of only water in the same beads, we see that the water signal associated with small T_2 values and strong internal gradients is still there, and that along the T_2 axis it is partly overlap-

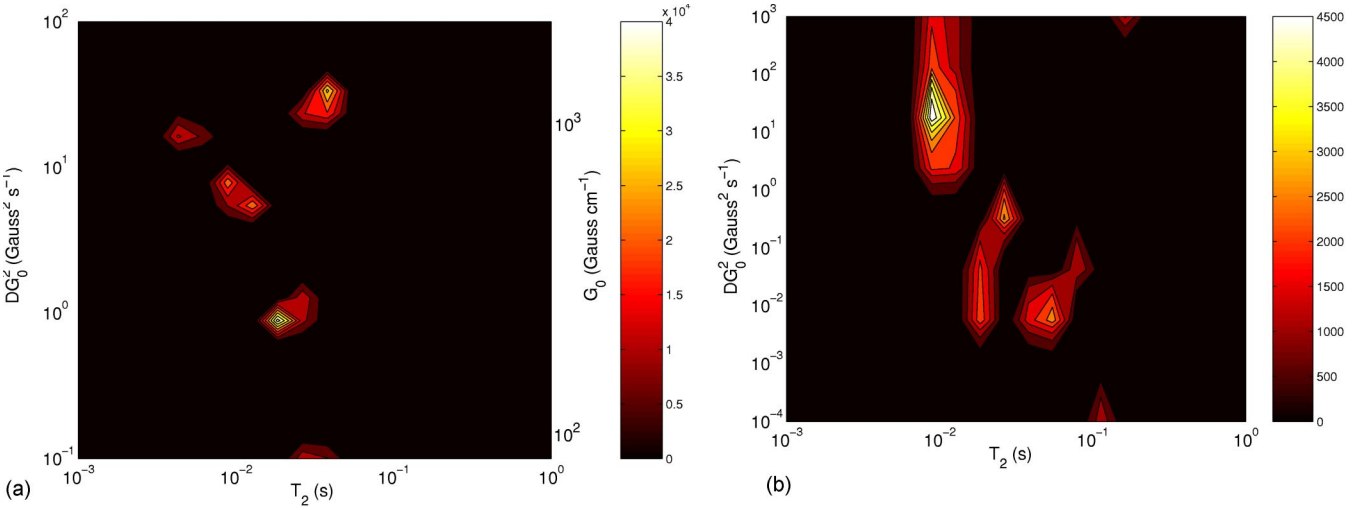

FIG. 7. (Color online) 2D distributions for T_2 and internal gradients of water and oil in water-wet glass beads. (a) Water in water-wet glass beads. (b) Water and oil in water-wet glass beads.

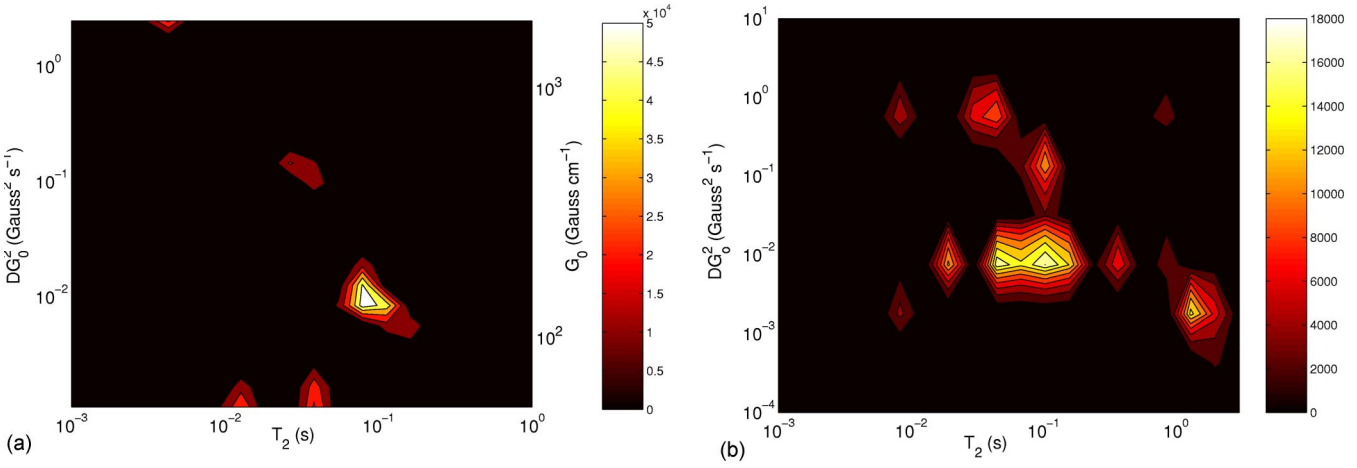

FIG. 8. (Color online) 2D distributions of T_2 and internal gradients for oil and water in oil-wet glass beads. (a) Oil in oil-wet glass beads. (b) Water and oil in oil-wet glass beads.

ping with the oil signal. Thus, using the dispersion effect from internal gradients it is possible to separate the signals from oil and water based on their difference in diffusivity and the internal gradients the molecules experience. If we normalize the vertical axis with respect to diffusion of oil (4×10^{-6} cm^2 s^{-1}), the oil peak will be associated with an internal gradient of around 100 G/cm. This is significantly lower than the water peak, which is associated with internal gradients in the range 300–1000 G/cm. This confirms that in this sample water is found close to the surface of the glass beads where the internal gradients are strongest, while the oil is found further away from the surface, in areas of lower internal gradients. In Fig. 8(a) we show the 2D "internal gradient–T_2" distribution of oil in oil-wet glass beads. Most of the oil signal is associated with an internal gradient around 200 G/cm, which is higher than observed for the oil signal in the water-wet glass beads. However, there is also some oil signal that has shorter T_2 values, and which is associated with internal gradients up to 1000 G/cm. When both oil and water are added to these oil-wet glass beads [Fig. 8(b)], we see that most of the signal is still found at the same place as observed in the sample with oil only, but some of the signal is somehow associated wih stronger internal gradients. In addition we see a peak at higher T_2 values, which we believe to be associated with water. However, we cannot clearly determine what part of the signal is water and what part is oil. The resolution along the vertical axis is not as good as it was in the water-wet beads. The reason is that in this oil-wet sample the products of diffusivity and the square of the internal gradients for oil and water have more similar values. This is due to the fact that one may expect most of the oil to be found in areas of relatively strong internal gradients, while most of the water is associated with areas of low or moderate strength of internal gradients.

In order to determine clearly what is water and what is oil in this oil-wet sample, we performed diffusion-weighted experiments, using the pulse sequence shown in Fig. 2. In Fig. 9(a) we see the total signal of oil and water in an experiment where the applied gradients are set equal to zero. If we compare this distribution with the one obtained without the diffusion encoding interval [Fig. 8(b)] we see that some of the signal associated with strong internal gradients is missing here. In Figs. 9(b) and 9(c) the separated oil and water signals are shown. We can clearly identify the main peaks observed in Fig. 9(a). Since we now have separated the signals from oil and water, we may normalize the vertical axis with the respective diffusion coefficients of oil and water. Most of the oil signal is associated with an internal gradient with a value around 200 G, as was also observed in the sample with only oil added. Some of the oil signal is also associated with stronger internal gradients. The water signal is located around a T_2 value of 1.4 s, and is associated with internal gradients of a strength of 10–50 G/cm, showing the bulklike behavior of water in this sample, and confirming that no water signals have T_2 values below 1 s.

If we compare the water-wet and oil-wet samples, we clearly see that the oil and water are found in areas having distinguishably different values of T_2 and internal gradients. In the water-wet sample the water is associated with relatively low T_2 values and strong internal gradients, while most of the oil signal is associated with longer T_2 values and lower internal gradients. In the oil-wet sample we see the opposite behavior, in particular for the water-signal. Here the water has a more bulklike behavior, with long T_2 values and low internal gradients. It is interesting to observe that the T_2 values of oil do not show such a pronounced difference in behavior for the two different samples. In both of the samples, the oil signal has a T_2 distribution with the main peak around 200 ms. However, in the oil-wet sample there is a shoulder stretching down to around 10 ms, which is not observed in the water-wet sample. In addition, the internal gradients are stronger in the oil-wet sample, although the difference in internal gradients is not as large as what is observed for the signal from water. This may be explained by the fact that the measured dephasing is dependent on the path the molecules travel through the field of internal gradients. Since the water molecules have much higher diffusivity than oil, they will probe a larger variety of the porous system, and thus also experience different values of internal gradients along their path. A larger portion of the water molecules will therefore experience areas of strong internal gradients, compared to the oil molecules, leading to an apparantly higher mean

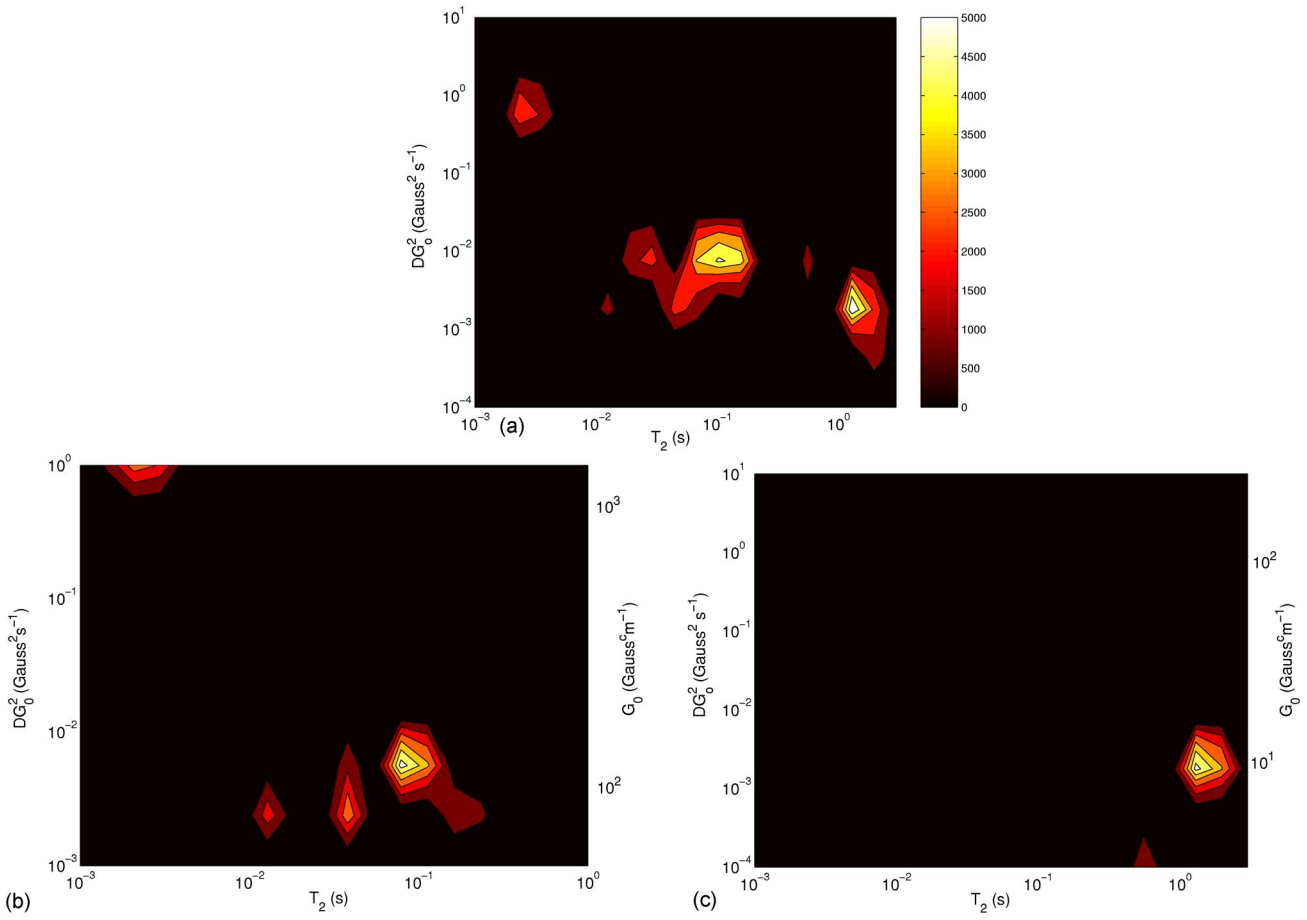

FIG. 9. (Color online) Diffusion separated 2D distributions for T_2 and internal gradients for oil and water in oil-wet glass beads. (a) With diffusion weighting interval, but with applied gradients equal to zero. (b) Separated oil signal. (c) Separated water signal.

value of measured internal gradients for water in the water-wet sample compared to oil in the oil-wet sample. In the oil-wet sample we observe that there is some portion of the oil molecules that experiences strong internal gradients, but the fraction is much lower than for water in the water-wet sample.

The results tell us that there are very strong internal gradients present in these glass spheres at this field strength. Figure 7(a) is a direct mapping of these internal gradients, and how they are correlated to the T_2 values of water. The strength of internal gradients varies between approximately 200 and 2000 G/cm.

Clearly, the wettability properties of the surface have the strongest influence on the signal of water. This is in agreement with results from experiments we have performed in rock cores [16] where we separated the T_2 distributions for oil and water based on their difference in diffusivity, and showed that the amount of bulk water present in the core may act as a good indicator of the wettability property of the surface of the rock material.

CONCLUSION

Due to the differences in magnetic susceptibility between liquid and solid material, strong internal gradients are induced when samples of glass beads immersed in oil and water are placed in a static magnetic field. We have shown that the distributions of internal gradients the different liquids experience in such systems can be correlated with the distributions of T_2 values. These correlations have been expressed as 2D diagrams of internal gradients and T_2 values. The wettability of the glass beads has a strong influence on the appearance of these diagrams, in particular on where the water signal is located. This can therefore be used as a diagnostic tool for the determination of the wettability properties of a liquid-filled porous material.

ACKNOWLEDGMENTS

We acknowledge financial support from the Norwegian Research Council. We also thank Professor Paul Callaghan for providing us with the 2D inverse Laplace software.

[1] H. C. Torrey, Phys. Rev. **104**, 563 (1956).
[2] R. F. Karlicek and I. J. Lowe, J. Magn. Reson. (1969-1992) **37**, 75 (1980).
[3] K. R. Brownstein and C. E. Tarr, Phys. Rev. A **19**, 2446 (1979).
[4] R. L. Kleinberg and M. A. Horsfield, J. Magn. Reson. (1969-1992) **88**, 9 (1990).
[5] H. Y. Carr and E. M. Purcell, Phys. Rev. **94**, 630 (1954).
[6] S. Meiboom and D. Gill, Rev. Sci. Instrum. **29**, 688 (1958).
[7] A. Sodickson and D. G. Cory, Prog. Nucl. Magn. Reson. Spectrosc. **33**, 77 (1998).
[8] B. Sun and K.-J. Dunn, Phys. Rev. E **65**, 051309 (2002).
[9] M. D. Hurlimann and L. Venkataramanan, J. Magn. Reson. **157**, 31 (2002).
[10] M. D. Hurlimann, L. Venkataramanan, and C. Flaum, J. Chem. Phys. **117**, 10 223 (2002).
[11] J. G. Seland, G. H. Sørland, H. W. Anthonsen, and J. Krane, Appl. Magn. Reson. **24**, 41 (2003).
[12] G. H. Sørland, D. Aksnes, and L. Gjerdåker, J. Magn. Reson. **137**, 397 (1999).
[13] P. T. Callaghan, S. Godefroy, and B. N. Ryland, J. Magn. Reson. **162**, 320 (2003).
[14] L. Venkataramanan, Y. Q. Song, and M. D. Hurlimann, IEEE Trans. Signal Process. **50**, 1017 (2002).
[15] Y. Q. Song, L. Venkataramanan, M. D. Hurlimann, M. Flaum, P. Frulla, and C. Straley, J. Magn. Reson. **154**, 261 (2002).
[16] G. H. Sørland, H. W. Anthonsen, J. G. Seland, F. Antonsen, H. C. Widerøe, and J. Krane, Appl. Magn. Reson. **26**, 417 (2004).